Enhanced Interferometric Identification of Spectra in Habitable Extra-Solar Planets

Eyal Schwartz, Stephen G. Lipson and Erez N. Ribak

Physics Department, Technion—Israel Institute of Technology, Haifa, Israel, 32000

An Earth-like extrasolar planet emits light that is many orders of magnitude fainter than that of the parent star. We propose a method of identifying bio-signature spectral lines in light of known extrasolar planets based on Fourier spectroscopy in the infrared, using an off-center part of a Fourier interferogram only. This results in superior sensitivity to narrower molecular-type spectral bands, which are expected in the planet spectrum but are absent in the parent star. We support this idea by numerical simulations that include photon and thermal noise, and show it to be feasible at a luminosity ratio of 10^{-6} for a Sun-like parent star in the infrared. We also carried out a laboratory experiment to illustrate the method. The results suggest that this method should be applicable to real planet searches.

Keywords: Astrobiology, Technique: interferometers, spectroscopic, Methods: observational, Planets and Satellites: detection, Infrared: planetary systems.

In this work, we propose a method of improving the chances of identifying a habitable Earth-like extrasolar planet using its spectral signature in the infrared. In Fourier transform spectroscopy (Bell 1972), the spectrum of a source is investigated using a two-beam interference pattern with variable path difference. A spectral feature (line or band) with center wavenumber k and width δk gives rise to oscillations having period 2π/k which decay within a path difference of ~1/δk. Thus, sharper spectral lines result in interferometric details at larger path differences. Moreover, from Parseval's theorem, which states that the energy in the interferogram due to a specific spectral feature is equal to that in the feature itself, a sharper line must correspond to a proportionally wider and weaker contribution to the interferogram in a given range. As a result, if we know in advance the range of line widths or bandwidths of spectral features which interest us, we can choose an appropriate part of the Fourier interferogram that optimizes the detectivity of such spectral features. In this way, available observing time can be used to collect the data most likely to be significant. For example, detection of the narrower line in Figure 1 will have a better signal-to-noise ratio (S/N) if we only measure the marked section (Ribak 2006). Similar interferometric techniques were implemented in other observational applications such as the Wind Imaging Interferometer (Shepherd et al. 1993).

An advantage of a Fourier spectrometer compared to a dispersion spectrometer (such as a multi-channel Echelle spectrograph) is that for this purpose it is not necessary to have specific information on center wavelengths of the bands expected because the molecules might have evolved differently than those on Earth. Most organic molecules have CH bonds which have absorption band widths of the order of 3 cm^{-1}, although the exact center wavelength depends on the bond strength and the molecular structure. A Fourier spectrometer can be designed to use the off-center region of the interferogram that is most sensitive to bands of this width, so that the S/N is improved significantly (Schwartz & Lipson 2011; Lipson et al. 2011). For example, in Earth's atmosphere the only common molecule with CH bonds is CH_4, which has an abundance of about 10^{-6}. As a result, concentrating the sampling to the interferogram region where bands of width 3 cm^{-1} dominate, we can perform a spectral analysis that has a significant advantage in sensitivity over straightforward Fourier spectroscopy using the complete interferogram. Since in general Fourier spectroscopy and dispersion spectroscopy have the same S/N when used with photon-limited detectors and negligible

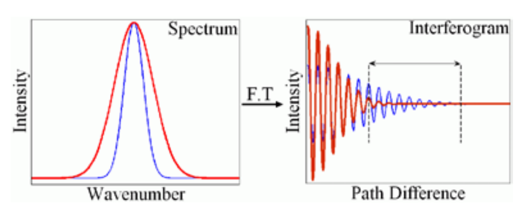

Figure 1. (Left) Two spectral features with a common central wave-number and different widths. (Right) The interferogram of both spectral features with the chosen part for differentiating the sharper narrow feature from the broad one.

broadband background radiation or detector noise, this method should show an advantage over dispersion spectroscopy, unless a very limited range of wavelengths is scanned in the available observation time. If detector noise is significant, Fourier spectroscopy has the known Fellgett advantage over dispersion spectroscopy (Bell 1972). We show below that the use of a cold field stop and adaptive optics can remove sufficient background radiation to make the system photon limited. An extension of the general idea could be applied to a more complex shape (e.g., a multiplet) for which an optimized sample of the interferogram could be defined.

We have studied in detail the application of the above proposal to the detection of bio-signatures in the spectrum of a star with an unresolvable planet, where the emission from the planet competes with the much stronger emission from the star. We consider the spectral signature of a star with a habitable extrasolar planet (exoplanet). This is expected to contain spectral details resulting from the star, from starlight reflected by the planet and from self-emission by the planet itself. If the planet has a bio-signature its reflectance and self-emission should contain molecular bands (Table 1).

Such spectra have been investigated extensively (Segura et al. 2003, 2005; Kaltenegger et al. 2007, 2010; Macdonald 1995), specifically in the mid-IR (3-24 μm; Gardner et al. 2006). The bio-signature spectra have relatively narrow bands, whereas in the same region the parent star has the broad spectrum of a black body with broader spectral features. Therefore, direct inspection of the interferogram at large enough path differences, where the transform of the spectral features resulting from the parent star have disappeared, can emphasize the existence of bio-signatures. However, the only narrow spectral features expected in the parent starlight are Fraunhofer lines with $\lambda < 1$ μm; therefore, the starlight must be filtered so as to exclude this part of the spectrum. It is beyond the scope of this work to delve into any specific model, so as a working example we take Earth-like molecules.

The bands shown in Table 1 lead to features in the interferogram out to path differences of $1/\delta k \sim 3$-5 mm. On the other hand, the parent star, as described above, will provide no features in the interferogram at path differences greater than several wavelengths. If the combined planet-star light is filtered by a long-pass filter with a gradual cutoff at around 5 μm, such bio-signatures will make a major contribution to the interferogram and will become dominant at path differences greater than about 10 μm. The gradual cutoff is necessary in order to avoid the introduction of high frequency features into the interferogram.

We have modeled such a system using the bio-signatures in Table 1 and also several spectral classes of parent stars. The

Table 1. Modeled extra solar bio-signature spectral lines for the mid-IR range

Molecule	Spectral line peak cm^{-1} (μm)	Spectral line width cm^{-1} (μm)
H_2O	512 (19.51)	2.66 (0.1)
N_2O	1285 (7.78)	2.2 (0.013)
CH_4	1280 (7.8)	2.86 (0.017)
O_3	1040 (9.6)	3.89 (0.036)
Chlorophyll a - $C_{55}H_{72}MgN_4O_5$	1478 (6.76)	3.5 (0.016)

results suggest that this method should be applicable to real planet searches. The long-pass filter is defined by an error function with a smooth enough cutoff which was calculated not to introduce artifacts in the interferogram. In order to fulfill the Nyquist criterion, we need to sample the interferogram at intervals of half of the shortest wavelength in the bands of interest, i.e., 6.76 μm. On the other hand, the total length of path difference to be sampled in order to get maximum resolution is about 2 mm. Therefore the number of sampling channels M is at most 600. However, a smaller number of channels could be used with a resultant degradation of the spectral resolution, down to a minimum of 60, which is needed to detect the longest wavelength in Table 1 with a resolving power of 10. The total photon flux is the sum of radiation from the exoplanet and parent star, emission from the telescope, atmospheric thermal radiation, and zodiacal light. The photon flux from the parent star depends on its apparent magnitude, m, the telescope aperture area, s, and the atmospheric transmittance, T (unless a space telescope is employed). We wish to estimate the number of photons accumulated per channel during an acceptable exposure time, t. The total number of photons N_{phs} received from the star is

$$N_{phs} = 2.51^{-m} tTsI_0 , \qquad (1)$$

where I_0 is the spectral irradiance from a zero-magnitude star in each of the standard spectral bands of the infrared range (M-Q bands) multiplied by the corresponding wavelength range (Labeyrie et al. 2006). The average number of photons received at any path difference in a Fourier spectrometer, N, assuming efficient optics and detectors in both exit ports of the interferometer, will be

$$N = N_{phs} + N_{php} + N_{tele} + N_{at} + N_{zl} , \qquad (2)$$

where N_{php} is the photon flux received from the planet, N_{tele} is the telescope thermal flux, N_{at} is atmospheric radiation, and N_{zl} are photons received from zodiacal dust scattering. Combining the above equations, considering N_{php} as the signal, gives a signal-to-noise in each of the M channels (Barducci et al. 2011 ; Maillard 1987)

$$SNR = N_{php}\left(NM\right)^{-0.5} \quad . \qquad (3)$$

where N_{php} is the photon flux received from the planet, N_{tele} is the telescope thermal flux, N_{at} is atmospheric radiation, and N_{zl} are photons received from zodiacal dust scattering. Combining the above equations, considering N_{php} as the signal, gives an S/N in each of the M channels (Barducci 2011; Barducci et al. 2010; Maillard 1987)

Two scenarios for such a contrast were studied. The first was a ground-based telescope such as the Very Large Telescope (VLT; Labeyrie et al. 2006; ESO Overview). The atmospheric noise was calculated based on the data from Lawrence et al. (2002) and the telescope emission as published for this telescope. The atmospheric transmission in each band is given by Labeyrie et al. (2006). Atmospheric emission was estimated as m = 3 arcsec^{-2} in the spectral region of interest (Lawrence et al. 2002), which makes a negligible contribution if adaptive optics and a cold field stop <0.25 arcsec^2 are used. Equation (3) shows that an S/N of 5 is obtained using M = 60 channels, an exposure time of $t \sim 10^5$ s and a contrast ratio $N_{php}/N_{phs} \sim 10^{-6}$. We thus find that the limiting magnitude of the parent star for which the proposed technique would succeed is m = 5 (Lena et al. 1998; Tokunaga 2000). This gives a limiting range of about 12 pc, or 40 light years, within which there are hundreds of stars of both classes. This estimate is based on star density statistics from our own solar neighborhood which states that about 18% of the stars within a 10 pc range are Sun-like (Henry et al. 2011). Some of these would be favorable for sustaining conditions for an Earth-like planet.

The second scenario was a space-based telescope like the *James Webb Space Telescope* (*JWST*; Gardner et al. 2006) for which we include the telescope emission and the Zodiacal light noise (Ootsubo et al. 2000). For this case we received a limiting parent star magnitude of m = 5 where T = 1 and S/N = 3.

We now turn to some simulations of the type of spectral signals expected. We chose ε Indi ($m \sim 2.2$) (Volk et al. 2003), as an example of a class K star within the parsec range described above. The habitable zone radius for an Earth-like planet revolving around this star is 0.2 AU (Kasting et al. 1993; Kaltenegger et al. 2010a, 2010b). We modeled the ground-based telescope VLT with the appropriate atmospheric and telescope noise. The parameters used were $t \sim 4 \times 10^4$ s, S/N = 5, M = 60 channels, atmospheric transmission T, modeled for each spectral band (Labeyrie et al. 2006) and s = 212 m^2.

Figure 2(a) shows in its entirety the interferogram obtained from the star chosen, treated as a blackbody with spectral features of the Sun (Renewable Resource Data Center, Solar Spectra), after applying a long-pass error-function filter as described in the figure caption. The spectral information in the interferogram has decayed after a few periods of oscillations. We confirmed that the long-pass filter makes no contribution to it. Figure 2(b) shows the selected region with a path difference of 3-5 mm, expanded to demonstrate the photon noise from the various sources as described above. Figure 2(c) shows an example of the selected region in Figure 2(b) when a habitable planet with contrast of 10^{-6} is added. The planet spectrum includes atmospheric-like gases and a chlorophyll molecular signature resulting from a major part of its surface.

To show that a bio-signature can be extracted reliably from such partial information we show in Figure the power spectrum derived by Fourier analysis using 60 measurement channels from the region of the interferogram of 3-5 mm path difference. It compares well with the original bio-spectrum (only the spectral lines themselves) despite the poor S/N of the signal itself. Based on simulations of this sort, we expect this method to provide information about the spectral signatures of possible exoplanet bio-molecules. Modulation of the bio-signature intensity and polarization as the planet rotates and orbits about the parent star might also be detectable and improve the S/N.

We ran an experiment using a simple breadboard Fourier spectrometer (Schwartz & Lipson 2011), which confirmed the ideas presented above. A 2 mm aperture was illuminated by an attenuated green Light Emitting Diode (LED) source superimposed on blackbody light from a halogen lamp. A comparison between the spectra retrieved from the entire interferogram and that retrieved from the selected part of the interferogram is shown in Figure 4. Although no attempt was

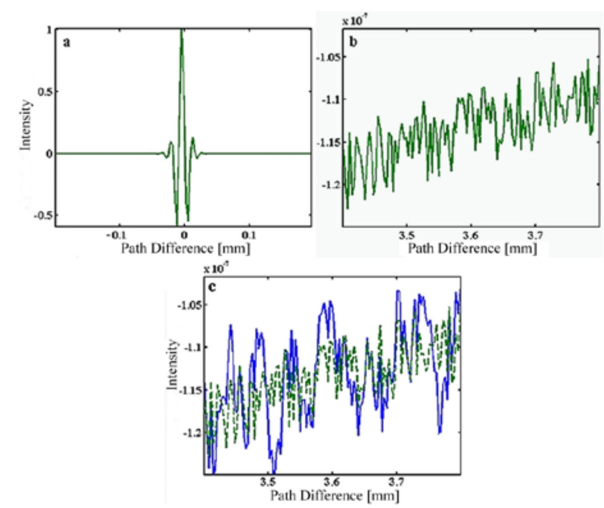

Figure 2: a) The interferogram of ε-Indi after applying a low-pass filter at 2000 cm^{-1} with error function profile σ =1200 cm^{-1}. b) Photon noise from the various sources in the selected path difference region. Exposure time on the VLT was t~4·10^4 s divided into 60 channels with SNR=5. c) Same noise as (b) including the planet bio-signature with 10^{-6} contrast.

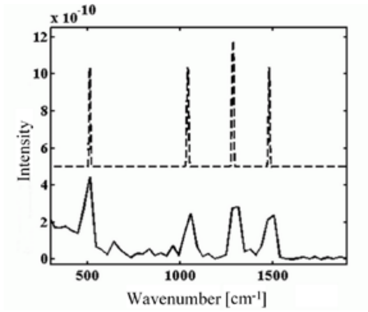

Figure 3. The bio-signature used before the addition of noise (above) and that reconstructed from the selected region of the interferogram with photon noise (below).

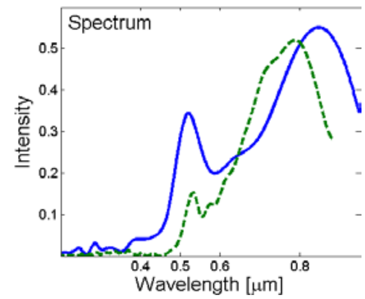

Figure 4. A fourfold contrast improvement is seen in this comparison between the spectra retrieved from the entire interferogram (green, dashed) and that retrieved from the selected part of the interferogram (blue).

made to optimize the optical setup it is clear from the figure that the relative signals from the LED and the black body have been improved.

An obstacle for this method might be that, if the telescope is situated on the ground, all radiation will be modulated by Earth's atmosphere itself. Moreover, fluctuations in the Earth atmosphere will result in variations in the apparent source position and intensity that may dominate the noise. One mitigation technique we implement is to use a double-output interferometer and subtract the two output signals to eliminate the unmodulated part (further correction of the intensity can be affected by dividing by the sum of the signals). We plan to use a zero-shear interferometer (Ribak et al. 1981) which is almost immune to turbulence, with a two-dimensional CCD. While a space telescope is the obvious solution to these problems, any method of significantly reducing Earth's spectral signature will help, such as a balloon platform or an Antarctic observatory, because of their reduced water-vapor contribution. Another possibility is to use a filter which only passes light in the known atmospheric windows where the molecular absorption by our atmosphere is negligible. Within such a window, the detection would then be restricted to the signature of chlorophyll-like and other molecules which are ground-based and must definitely be attributed to the planet.

In summary, we have proposed a method of differentiating between spectral bands of different widths by optimized sampling of their Fourier interferograms. We tested it by simulations related to detecting possible habitable extrasolar planets using their spectral bio-signatures, in the presence of overwhelming parent star radiation and different noise sources. Also, we conducted a laboratory experiment that illustrated the method using two light sources. We showed that, using adaptive optics and a cold aperture, the background radiation can be reduced sufficiently that the method will be applicable to stars with limiting magnitudes of $m = 5$ at a distance of 12 pc for the VLT and for the future *JWST* space-based telescope. This method could also have applications outside astrophysics. Another method that could be implemented parallel to the one we suggest here is temporal modulation of the interference pattern, which will take the atmospheric turbulence influence to be even lower, thus allowing a shorter exposure time in order to achieve an adequate S/N.

We are grateful for useful experimental assistance and input from Dr. D. Spector, N. Meitav, and S. Hoida. E.S. acknowledges financial support from the Asher Space Institute at Technion. Parts of this work were supported by the Israel Science Foundation and the Ministry of Science.

References

Barducci, A. 2011, J. Opt. Soc. Am. B, 28, 637
Barducci, A., Guzzi, D., & Lastri, C. et al. 2010, Opt. Exp., 18, 11622
Bell, R. J. 1972, Introductory Fourier Transform Spectroscopy (New York: Academic)
Gardner, J. P., Mather, J. C., & Clampin, M. et al. 2006, Space Sci. Rev., 123, 485
Henry, T., Chatelain, J., & Davison, C. et al. 2011, EPSC-DPS2011-656-1, Vol. 6
Kaltenegger, L., Eiroa, C., & Fridlund, M. 2010a, Ap&SS, 326, 233
Kaltenegger, L., Selsis, F., & Fridlund, M. et al. 2010b, Astrobiology, 10, 1
Kaltenegger, L., Traub, W. A., & Jucks, K. W. 2007, ApJ, 658, 598
Kasting, J. F., Whitmire, D. P., & Reynolds, R. T. 1993, Icarus, 101, 108
Labeyrie, A., Lipson, S. G., & Nisenson, P. 2006, An Introduction to Optical Stellar Interferometry (Cambridge: Cambridge Univ. Press), 316
Lawrence, J. S., Ashley, M. C. B., Burton, M. G., & Storey, J. W. V. 2002, Proc. SPIE, 4836, 176
Lena, P., Lebrun, F., & Mignard, F. 1998, Observational Astrophysics, 2nd ed. (Berlin: Springer), 91

Lipson, A., Lipson, S. G., & Lipson, H. 2011, Optical Physics, 4th ed. (Cambridge: Cambridge Univ. Press), 374
Lipson, S. G. & Schwartz, E. 2011, Applied Industrial Optics: Spectroscopy, Imaging and Metrology, OSA Technical Digest (CD) (Washington, DC: Optical Society of America), paper JWA5 (http://www.opticsinfobase.org/abstract.cfm?URI=HISE-2011-JWA5)
Macdonald, G. M., Steenhuis, J. J., & Barry, B. A. 1995, J. Biol. Chem., 270, 15
Maillard, J. P. 1987, Signal-To-Noise Ratio and Astronomical Fourier Transform Spectroscopy, Vol. 132 (Dordrecht: Kluwer), 71
Ootsubo, T., Onaka, T., & Yamamura, I. et al. 2000, Adv. Space Res., 25, 2163
Ribak, E. N. 2006, Proc. SPIE, 6268, 62683G
Ribak, E. N. & Lipson, S. G. 1981, Appl. Opt., 20, 1102
Schwartz, E. & Lipson, S. G. 2011, OSA Technical Digest (CD) (Washington, DC: Optical Society of America), paper JPDP4 (http://www.opticsinfobase.org/abstract.cfm?URI=FTS-2011-JPDP4)
Segura, A., Krelove, K., & Kasting, J. F. et al. 2003, Astrobiology, 3, 689
Segura, A., Krelove, K., & Kasting, J. F. et al. 2005, Astrobiology, 5, 706
Shepherd, G. G., Thuillier, G., & Gault, W. A. et al. 1993, J. Geophys. Res., 98, 10725
Tokunaga, A. T. 2000, Allen's Astrophysical Quantities, 4th ed., ed. A. N. Cox (New York: Springer), 143
Volk, K., Blum, R., Walker, G., & Puxley, P. 2003, IAU Circ., 8188, 2